Smamite, Ca₂Sb(OH)₄[H(AsO₄)₂]·6H₂O, a new mineral and a possible sink for Sb during weathering of fahlore

Jakub Plášil[1,*], **Anthony R. Kampf**[2], **Nicolas Meisser**[3], **Cédric Lheur**[4],
Thierry Brunsperger[5], and **Radek Škoda**[6,†]

[1]Institute of Physics ASCR, v.v.i., Na Slovance 1999/2, 18221 Prague 8, Czech Republic
[2]Mineral Sciences Department, Natural History Museum of Los Angeles County, 900 Exposition Boulevard, Los Angeles, California 90007, U.S.A.
[3]Musée cantonal de géologie, Université de Lausanne, Anthropole, Dorigny, CH-1015 Lausanne, Switzerland
[4]1 rue du St. Laurent, 54280 Seichamps, France
[5]22 route de Wintzenheim, 68000 Colmar, France
[6]Department of Geological Sciences, Faculty of Science, Masaryk University, Kotláøská 2, 611 37, Brno, Czech Republic

Abstract

Smamite, Ca₂Sb(OH)₄[H(AsO₄)₂]·6H₂O, is a new mineral species from the Giftgrube mine, Rauenthal, Sainte-Marie-Aux-Mines ore-district, Haut-Rhin department, France. It is a supergene mineral found in quartz-carbonate gangue with disseminated to massive tennantite-tetrahedrite series minerals, native arsenic, Ni-Co arsenides, and supergene minerals picropharmacolite, fluckite, and pharmacolite. Smamite occurs as lenticular crystals growing in aggregates up to 0.5 mm across. The new mineral is whitish to color-less, transparent with vitreous luster and white streak; non-fluorescent under UV radiation. The Mohs hardness is ~3½; the tenacity is brittle, the fracture is curved, and there is no apparent cleavage. The measured density is 2.72(3) g/cm³; the calculated density is 2.709 g/cm³ for the ideal formula. The mineral is insoluble in H₂O and quickly soluble in dilute (10%) HCl at room temperature. Optically, smamite is biaxial (–), α = 1.556(1), β = 1.581(1), γ = 1.588(1) (white light). The $2V$ (meas) = 54(1)°; $2V$ (calc) = 55.1°. The dispersion is weak, $r > v$. Smamite is non-pleochroic. Electron microprobe analyses provided the empirical formula Ca₂.₀₃Sb₀.₉₇(OH)₄[H₁.₁₀(As₁.₉₉Si₀.₀₁O₄)₂]·6H₂O. Smamite is triclinic, $P\bar{1}$, a = 5.8207(4), b = 8.0959(6), c = 8.21296(6) Å, α = 95.8343(7)°, β = 110.762(8)°, γ = 104.012(7)°, V = 402.57(5) Å³, and Z = 1. The structure (R_{obs} = 0.027 for 1518 $I > 3\sigma I$ reflections) is based upon {Ca₂(H₂O)₆Sb(OH)₄[H(AsO₄)₂]} infinite chains consisting of edge-sharing dimers of Ca(H₂O)₃O₂(OH)₂ polyhedra that share edges with Sb(OH)₄O₂ octahedra; adjacent chains are linked by H-bonds, including one strong, symmetrical H-bond with an O–H bond-length of ~1.23 Å. The name "smamite" is based on the acronym of the Sainte-Marie-aux-Mines district.

Keywords: Smamite, new mineral species, arsenate, crystal structure, weathering, fahlore, Sainte-Marie-aux-Mines

Introduction

Oxidative weathering of base-metal ore deposits containing complex sulfide and sulfosalt minerals leads potentially to a release of significant amounts of heavy metals and metalloids, especially As, Pb, Bi, or Sb into the environment. Supergene minerals formed during weathering in oxidation zones of these deposits, then served as a temporary or final sink for toxic elements otherwise released into the groundwater. Therefore, an exact knowledge of the supergene mineralogy of a particular deposit is of great importance as it can be used to assess and predict the behavior and mobility of elements during weathering, both natural or anthropogenically induced (e.g., Borčinová Radková et al. 2017; Keim et al. 2018; Majzlan et al. 2018; Đorđević et al. 2019, and references therein). Smamite, a new hydrated arsenate mineral containing Sb(V) as an essential component, is formed via oxidative weathering of a complex hypogene mineral association at Sainte-Marie-Aux-Mines district (France) in the conditions of the old mine workings. Although it is currently

known only from a few specimens, it is likely to be much more common, having been overlooked due to its inconspicuous appearance. Therefore, it may prove to be another important sink for antimony in supergene weathering assemblages.

The new mineral is based on the acronym "SMAM" for the type locality, the famous Sainte-Marie-Aux-Mines polymetallic mining district, in Haut-Rhin department, France. The mining district of Sainte-Marie is known both for its long-lasting mining activities in the past and for its interesting mineralogy. It has yielded nine new arsenate mineral species: ferrarisite (Bari et al. 1980a), fluckite (Bari et al. 1980b), mcnearite (Sarp et al. 1981), phaunouxite (Bari et al. 1982), rauenthalite (Pierrot 1964), sainfeldite (Pierrot 1964), villyaellenite (Sarp 1984), weilite (Herpin and Pierrot 1963), and giftgrubeite (Meisser et al. 2019). The new mineral and name were approved by the Commission on New Minerals, Nomenclature and Classification of the International Mineralogical Association (IMA 2019-001). One holotype and two co-type specimens are deposited in the Mineralogical Collection of the Musée cantonal de géologie, University of Lausanne, Anthropole, Dorigny, CH-1015 Lausanne, Switzerland, with the catalog numbers MGL no. 093481, 093482,

---

* E-mail: plasil@fzu.cz. Orcid 0000-0001-6627-5742.
† Orcid 0000-0001-6097-4294.

and 093483, respectively. One co-type specimen is deposited in the mineral collections of the Natural History Museum of Los Angeles County, under catalog number 67169.

OCCURRENCE

Smamite was found in the Giftgrube mine, which exploits the famous St. Jacques vein rich in arsenic, in Rauenthal, Sainte-Marie-Aux-Mines, Haut-Rhin department, Grand Est, France. It is a supergene mineral resulting from the weathering of primary As-mineralization (mainly consisting of native arsenic, tennantite-tetrahedrite, arsenides of Co and Ni, and löllingite and chalcopyrite) in the old mine workings. The supergene minerals associated with smamite include picropharmacolite, fluckite, pharmacolite, quartz, and carbonates (calcite and dolomite). The Giftgrube mine was apparently first mined in the 16th century and some galleries were reopened later, especially during the 18th century. The Giftgrube mine is also the type locality for the recently discovered mineral giftgrubeite (Meisser et al. 2019).

PHYSICAL AND OPTICAL PROPERTIES

Crystals of smamite are lenticular in shape, forming aggregates up to about 0.5 mm in size (Figs. 1 and 2). The mineral is white to colorless, transparent with vitreous luster and white streak. Smamite is nonfluorescent in long- or short-wave ultraviolet light. It has a Mohs hardness of about 3½, a brittle tenacity, curved fracture, and no apparent cleavage. The density measured by flotation in a mixture of diiodomethane/1-chloronaphtalene (23.5 °C; $n = 3$) is 2.72(3) g/cm³. The calculated density is 2.690 g/cm³ for the empirical formula and 2.709 g/cm³ for the ideal formula. The mineral is insoluble in H_2O and quickly soluble in dilute (10%) HCl at room temperature. After H_2O dilution of the HCl solution, a white Sb-oxychloride precipitate slowly forms.

Smamite is optically biaxial (–) with indices of refraction $\alpha = 1.556(1)$, $\beta = 1.581(1)$, $\gamma = 1.588(1)$ measured in white light. The $2V$ measured using extinction data analyzed with EXCALIBRW (Gunter et al. 2004) is 54(1)°; the calculated $2V$ is 55.1°. The dispersion is weak, $r > v$. The optical orientation was not determined. Smamite is non-pleochroic. The Gladstone–Dale compatibility, $1 - (K_P/K_C)$, (Mandarino 2007) is –0.014 (superior) using the empirical formula.

Raman spectroscopy

Raman spectroscopy was conducted on a Jobin-Yvon Labram HR Evolution system, using a 600 lines/mm grating and a He–Ne 633 nm laser with a beam power of 10 mW at the sample surface. The spectrum was collected from 4000 to 100 cm⁻¹ (Fig. 3). Band fitting was done after appropriate background correction, assuming combined Lorentzian-Gaussian band shapes using the Voigt function (PeakFit; Jandel Scientific Software).

The Raman spectrum is dominated by the stretching vibrations of AsO_4 tetrahedra. The broad, but resolved band (~3500–3000 cm⁻¹) consisting of several overlapping bands (3510, 3433, 3384, 3521, 3148 cm⁻¹) corresponds to O–H stretching vibrations. According to the correlation given by Libowitzky (1999), these vibrations correspond to H-bonds (H···*Acceptor*) in the range 2.1–1.7 Å. These values are in line with those obtained from the structure determination. There are no bands that can be reliably assigned to the ν_2 (δ) H–O–H as it is overlapped by strong fluorescence. The overlapping composite band of medium intensity composed of bands at 892, 870, 850, and 826 cm⁻¹ is attributed to ν_3 antisymmetric and the ν_1 symmetric As–O vibrations of the As-tetrahedra. A shoulder at 788 cm⁻¹ is most probably related to the out-of-plane bending vibration of the Sb–O-H. A sharp band of highest intensity, at 642 cm⁻¹, is probably related to the antisymmetric stretching vibration of the O–Sb–O–As–O linkage in [$Sb(OH)_4O_2(AsO_4)$] fragments. Bands of low intensity at 585, 547, and 510 cm⁻¹ are overlapping Sb–O stretching vibrations of $Sb(OH)_4O_2$ and ν_4 (δ) O–As–O tetrahedra. Bands of low intensity at 418, 401, 372, 339, 289, and 254 cm⁻¹ and two bands with high intensity at 234 and 212 cm⁻¹ are related to ν_2 (δ) O–As–O bending vibrations and various bending H-O–Sb and H–O–As vibrations. The bands at the lowest energies are due to phonons.

FIGURE 1. Lenticular crystals of smamite from Giftgrube mine, Sainte-Marie-Aux-Mines. Horizontal field of view is 0.6 mm (photo W. Perraud). (Color online.)
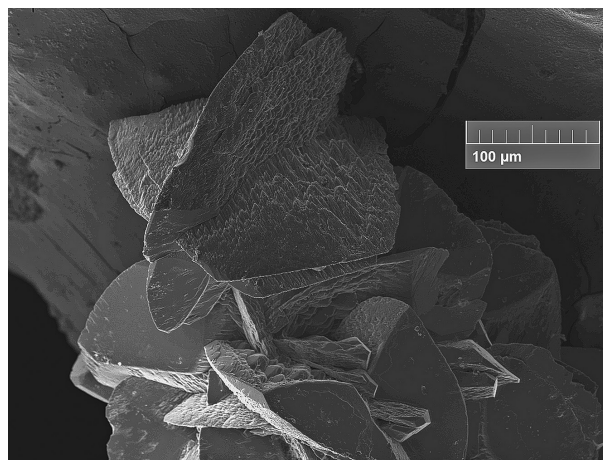

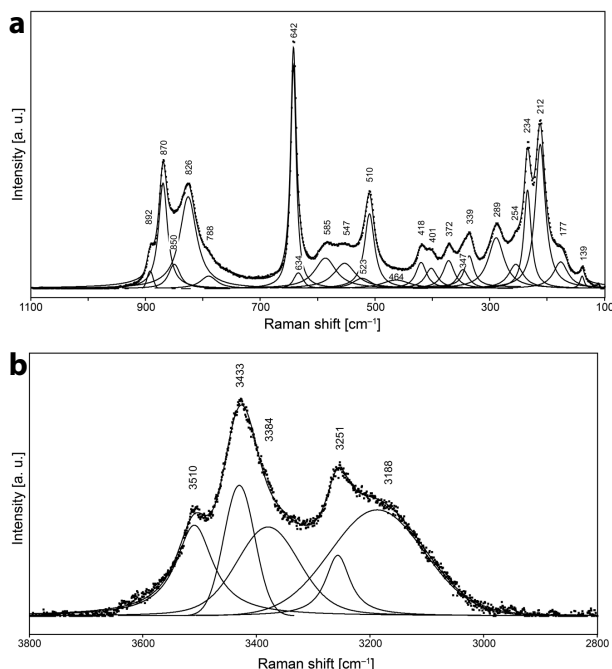**FIGURE 2.** Aggregate of smamite crystals with apparently stepped faces. SE image (photo C. Lheur).

TABLE 1. Analytical results for smamite (wt%)

Constituent	Mean	Range	St.dev.	Probe standard
CaO	17.34	17.07–17.72	0.30	andradite
Sb$_2$O$_5$	23.92	22.33–25.62	1.29	metallic Sb
SiO$_2$	0.12	0.00–0.20	0.08	sanidine
As$_2$O$_5$	34.93	33.69–36.44	1.49	lammerite
H$_2$O[a]	23.50			
Total	99.81			

[a] Based on structure.

the application of an empirical absorption correction using the multi-scan method with ABSCOR (Higashi 2001). The structure was solved using SHELXT program (Sheldrick 2015) and was refined by the least-squares algorithm in Jana2006 (Petříček et al. 2014) based on F^2. Some of the O atoms and, in particular, the H atoms were located from the difference Fourier maps. The H atoms were refined with soft constraints on the O–H distances and U_{iso} of the H atoms were set at 1.2 times that of the corresponding donor O atom. The refinement converged smoothly to R = 0.0274 and wR = 0.0679 for 1518 unique observed reflections (GOF = 1.68) (Supplemental[1] Table S2). Atom coordinates and displacement parameters are listed in Tables 2 and 3; selected interatomic distances and a bond-valence analysis are provided in Tables 4 and 5, respectively.

DESCRIPTION OF THE STRUCTURE

Smamite has a unique structure (Figs. 4a and 4b), with several remarkable features (see below). The structure contains one Sb, one Ca, one As, nine H, and nine O atoms in the asymmetric unit (all atoms occupying 2i sites, except Sb and H5, which occupy 1g and 1d sites, respectively). The Sb site is coordinated as a regular octahedron in which the four equatorial vertices are OH groups (two symmetrically related sites OH2 and OH3) and the two apical apices (related by an inversion center) are O atoms (O1 and O1′). The occupancy of the Sb site refined to less than unity. The Ca site is sevenfold-coordinated by two O atoms, two OH groups, and three H$_2$O groups (Table 4). The As^{5+} is coordinated as a regular tetrahedron by three O atoms, while the fourth vertex of the tetrahedron is protonated (linking the H5 atom, see below). The structure is based upon {Ca$_2$(H$_2$O)$_6$Sb(OH)$_4$[H(AsO$_4$)$_2$]} infinite chains running approximately parallel to [110]. These chains result from edge-sharing dimers of Ca(H$_2$O)$_3$O$_2$(OH)$_2$ polyhedra that in turn share edges with Sb(OH)$_4$O$_2$ octahedra. The chain is decorated by AsO$_4$ tetrahedra pointing up and down along the length of the chain (Fig. 5). Adjacent chains are linked by H-bonds. There is a particularly interesting short, symmetrical H-bond, O5–H5–O5′ (Fig. 3a) with an O–H bond-length of ~1.23 Å. Such strong, symmetrical H-bond has been already reported in structures of arsenate minerals and compounds (Ferraris et al. 1971, 1972; Ondruš et al. 2013). These H-bonds have an O-H bond-length of ~1.22 Å. Considering the refined site occupancies and the bond-valence sums, the structural formula for smamite is Ca$_2$(H$_2$[3]O)$_4$(H$_2$[4]O)$_2$Sb$_{0.94}$(OH)[H(AsO$_4$)$_2$], Z = 1. We note that this formula has a net charge of –0.3 due to a 0.06 deficiency in the Sb^{5+} occupancy. However, we cannot be certain that the deficit in Sb occupancy is real or is an artifact perhaps caused by an inadequate absorption correction. If it is real, it could be compensated by additional protonation of the arsenate group.

Chemical analysis

Smamite was analyzed in a polished section with a Cameca SX-100 electron microprobe operating in wavelength-dispersive spectroscopy (WDS) mode using 15 kV accelerating voltage, 4 nA beam current and a beam diameter of 10 μm. Raw X-ray intensities were corrected for matrix effects with a φρ(z) algorithm of X-PHI routine (Merlet 1994). Because insufficient material was available for a direct determination of H$_2$O, the amount of water was calculated on the basis of stoichiometry (5 total cations pfu, 18 O apfu, and charge balance) as indicated by the structure. Analytical data are given in Table 1. The empirical formula is Ca$_{2.03}$Sb$_{0.97}$(OH)$_4$[H$_{1.10}$(As$_{1.99}$Si$_{0.01}$O$_4$)$_2$]·6H$_2$O. The ideal formula is Ca$_2$Sb(OH)$_4$[H(AsO$_4$)$_2$]·6H$_2$O, which requires CaO 17.07, Sb$_2$O$_5$ 24.63, As$_2$O$_5$ 34.99, H$_2$O 23.31, total 100 wt%.

X-ray crystallography and structure determination

Both powder and single-crystal X-ray studies were carried out using a Rigaku R-Axis Rapid II curved imaging plate micro-diffractometer with monochromatized MoKα radiation. For the powder study, a Gandolfi-like motion geometry on the φ and ω axes was used to randomize the sample. Observed d values and intensities were derived by profile fitting using JADE 2010 software. Data are given in Supplemental[1] Table S1. Triclinic unit-cell parameters refined from the powder data using JADE 2010 with whole pattern fitting are a = 6.822(5), b = 8.094(5), c = 8.218(5) Å, α = 95.80(2)°, β = 110.77(2)°, γ = 104.94(2)°, and V = 403.0(2) Å^3.

A small 90 × 90 × 40 μm fragment of adequate crystal quality was chosen for the data collection; details are given in Supplemental[1] Table S2. The Rigaku CrystalClear software package was used for processing the structure data, including

FIGURE 3. Raman spectrum of smamite with fitted band components: (**a**) in the range 1100–100 cm^{-1}, (**b**) 3800–2800 cm^{-1}.

TABLE 2. Atom coordinates and displacement parameters (Å²) for smamite

Atom	x	y	z	U_{eq}/U_{iso}	U^{11}	U^{22}	U^{33}	U^{12}	U^{13}	U^{23}
Sb[a]	0	0.5	0.5	0.01387(16)	0.0132(2)	0.0121(2)	0.0149(2)	0.00122(16)	0.00599(16)	0.00111(15)
As	0.51277(7)	0.23744(5)	0.22317(5)	0.01522(17)	0.0158(2)	0.0135(2)	0.0154(2)	0.00347(17)	0.00597(17)	0.00171(16)
Ca	0.74579(13)	0.16429(10)	0.66895(10)	0.0184(3)	0.0173(5)	0.0167(4)	0.0173(4)	0.0017(3)	0.0048(3)	0.0025(3)
O1	0.7736(4)	0.3645(4)	0.2626(4)	0.0211(12)	0.0170(16)	0.0204(15)	0.0224(16)	−0.0018(12)	0.0096(13)	0.0007(12)
OH2	0.7822(5)	0.4487(4)	0.5989(4)	0.0217(12)	0.0238(17)	0.0150(14)	0.0275(16)	−0.0017(13)	0.0158(13)	−0.0011(12)
H2	0.730(7)	0.534(4)	0.648(5)	0.026[b]						
OH3	0.9583(5)	0.7212(4)	0.4473(4)	0.0220(12)	0.0172(16)	0.0204(15)	0.027(17)	0.0062(13)	0.0068(13)	0.0064(13)
H3	0.812(3)	0.709(6)	0.366(4)	0.0264[b]	0.0212(16)	0.0186(14)	0.0155(14)	−0.0006(12)	0.0054(12)	0.0051(12)
O4	0.5202(5)	0.0997(4)	0.3617(3)	0.0201(11)	0.0270(17)	0.0193(15)	0.0148(14)	0.0068(13)	0.0063(13)	−0.0010(11)
O5	0.4258(5)	0.1223(4)	0.0130(4)	0.0213(12)	0.0217(16)	0.0205(15)	0.0265(16)	0.0119(13)	0.0092(13)	0.0039(13)
O6	0.3550(5)	0.3657(3)	0.2154(4)	0.0220(12)	0.0291(18)	0.0221(16)	0.0280(17)	0.0045(14)	0.0147(14)	0.0048(13)
Ow7	0.4754(5)	0.2829(4)	0.7455(4)	0.0260(13)	0.0212(16)	0.0186(14)	0.0155(14)	−0.0006(12)	0.0054(12)	0.0051(12)
H7a	0.539(7)	0.406(2)	0.772(6)	0.0312[b]						
H7b	0.470(7)	0.244(6)	0.849(4)	0.0312[b]						
Ow8	0.9869(5)	0.9862(4)	0.7410(4)	0.0340(15)	0.030(2)	0.0296(19)	0.038(2)	0.0132(16)	0.0066(16)	0.0038(16)
H8a	1.124(5)	1.024(6)	0.844(4)	0.0408[b]						
H8b	0.987(8)	0.915(5)	0.638(4)	0.0408[b]						
Ow9	0.9350(6)	0.2801(5)	0.9757(4)	0.0413(16)	0.029(2)	0.064(2)	0.0234(19)	0.0203(19)	0.0016(15)	−0.0052(17)
H9a	1.090(3)	0.305(7)	1.049(6)	0.0496[b]						
H9b	0.852(7)	0.318(6)	1.038(6)	0.0496[b]						
H5	0.5	0	0	0.0256[b]						

[a] Refined occupancy 0.9376(13).
[b] Refined with isotropic displacement parameter.

TABLE 3. Selected interatomic distances (Å) for smamite

Sb-O1[i]	2.000(2)	Ca-Oh2	2.406(3)
Sb-O1[ii]	2.000(2)	Ca-Oh3[v]	2.546(4)
Sb-Oh2[i]	1.914(4)	Ca-O4	2.366(2)
Sb-Oh2[ii]	1.914(4)	Ca-O4[vi]	2.369(3)
Sb-Oh3[i]	1.947(3)	Ca-Ow7	2.505(4)
Sb-Oh3[ii]	1.947(3)	Ca-Ow8[vii]	2.401(4)
<Sb-O>	1.95	Ca-Ow9	2.350(3)
		<Ca-O>	2.42
As-O1	1.722(3)		
As-O4	1.669(3)		
As-O5	1.697(3)		
As-O6	1.657(3)		
<As-O>	1.69		

Notes: Symmetry codes: (1) x−1, y, z; (2) −x+1, −y+1, −z+1; (3) x, y, z−1; (4) x−1, y, z−1; (5) −x+2, −y+1, −z+1; (6) −x+1, −y, −z+1; (7) x, y−1, z; (8) −x+2, −y+1, −z+2; (9) −x+2, −y+2, −z+1; (x) −x+1, −y, −z; (xi) x−1, y−1, z−1; (xii) x−1, y−1, z; (xiii) x, y, z+1; (xiv) x, y+1, z; (xv) x+1, y+1, z+1.

TABLE 4. Hydrogen-bond geometry (in Å, °) in the structure of smamite

D–H···A	D–H	H···A	D···A	D–H···A
Oh2-H2···O6[ii]	0.96(5)	1.66(5)	2.586(5)	159(4)
Oh3-H3···Ow7[ii]	0.96(2)	1.87(3)	2.807(4)	166(3)
Ow7-H7a···O6[ii]	0.953(16)	1.792(19)	2.737(4)	171(4)
Ow7-H7b···O5[xiii]	0.95(4)	1.81(4)	2.743(5)	167(3)
Ow8-H8a···O5[xv]	0.97(3)	1.94(3)	2.886(4)	167(3)
Ow8-H8b···Oh3	0.97(4)	2.02(4)	2.978(5)	167(4)
Ow9-H9a···O6[xvi]	0.97(2)	1.75(2)	2.707(4)	168(4)
Ow9-H9b···O1[xiii]	0.97(6)	2.12(6)	3.018(5)	154(4)
O5-H5···O5[x]	1.228(4)	1.228(4)	2.455(5)	180

Notes: Symmetry codes: (ii) −x+1, −y+1, −z+1; (x) −x+1, −y, −z; (xiii) x, y, z+1; (xv) x+1, y+1, z+1; (xvi) x+1, y, z+1.

There is no mineral structurally similar to smamite. The presence of both Sb^{5+} and As^{5+} suggests strongly oxidizing conditions of formation. Richelsdorfite (Süsse and Tillmann 1987) and joelbruggerite (Mills et al. 2009) also contain both Sb^{5+} and As^{5+}, but their structures are completely different than that of smamite. Another recently approved Ca-, Sb- and As-containing mineral, pracharite, $CaSb_2^{5+}(As_2^{3+}O_5)_2O_2 \cdot 10H_2O$ (Kolitsch et al. 2018), contains trivalent arsenic and a structure that is quite distinct.

IMPLICATIONS

The new mineral smamite was formed via supergene oxidative weathering of a complex mineral assemblage including fahlore (minerals of the tetrahedrite-tennantite series), Ni-As minerals, and native arsenic. The evolution of the supergene association is likely to have involved several steps. The first step is probably the oxidation of massive or disseminated native arsenic and the formation of As_2O_3, which is thermodynamically favored (Majzlan et al. 2014). The As_2O_3 oxidizes in contact with humid air or descending (meteoric) water, yielding strongly acidic solutions containing As^{5+} as various hydrogenarsenate anions, e.g., $(H_2AsO_4)^-$ and $(HAsO_4)^{2-}$ (cf. Majzlan et al. 2014). Such solutions then attack gangue carbonates, here mostly Mn–Fe bearing calcite and dolomite, and partly oxidized tennantite-tetrahedrite (fahlore), which shifts the pH to more alkaline (cf. model 3Aa of Markl et al. 2014), and this results in the deposition of smamite (as the only Ca-bearing antimonate-arsenate), picropharmacolite (as the main Mg-bearing arsenate),
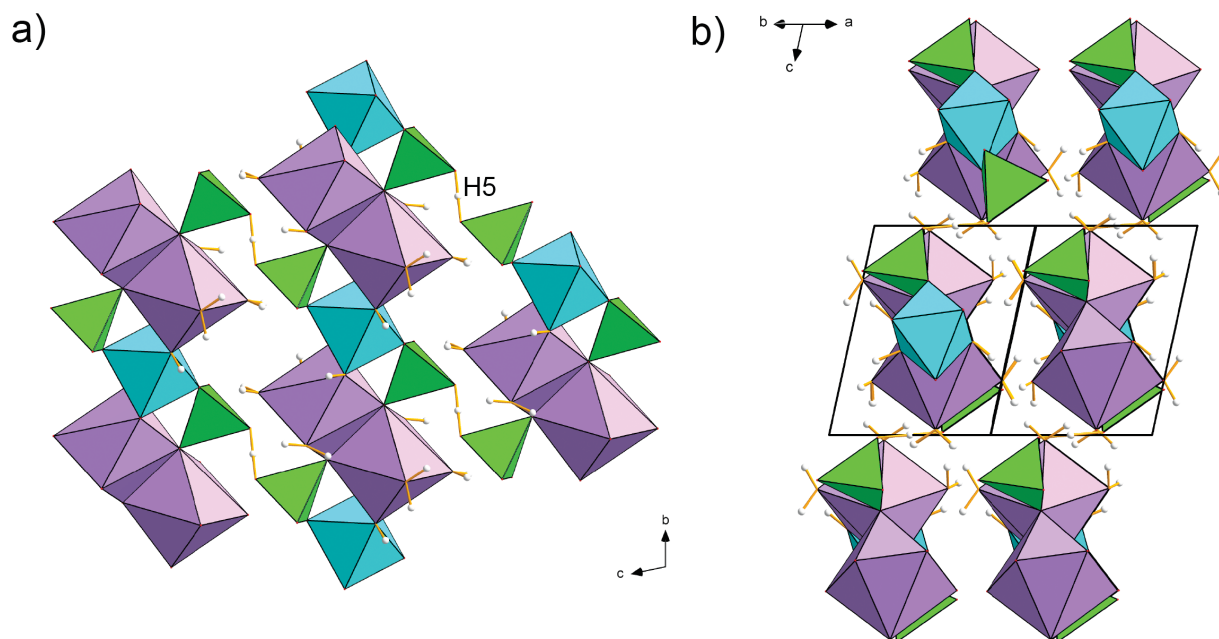
TABLE 5. The bond-valence analysis for smamite[a]

	Sb	Ca	As	H2	H3	H5	H7a	H7b	H8a	H8b	H9a	H9b	ΣBV
O1	0.80 ×2↓		1.13									0.06	1.99
Oh2	0.95 ×2↓	0.30		0.89									2.14
Oh3	0.89 ×2↓	0.21			0.91					0.08			2.08
O4		0.33, 0.32	1.31										1.96
O5			1.21			0.48 ×2↓		0.12	0.09				1.91
O6			1.36	0.18			0.13				0.14		1.81
Ow7		0.23			0.11		0.92	0.93					2.19
Ow8		0.30							0.89	0.89			2.07
Ow9		0.34									0.89	0.89	2.11
ΣBV	5.28	2.02	5.02	1.07	1.01	0.97	1.05	1.05	0.98	0.96	1.03	0.95	

[a] All values are in valence units (v.u.); ×2↓ = multiplicity; ΣBV = sum of the bond-valences; bond-valence parameters were taken from Gagné and Hawthorne (2015) (Sb^{5+}–O, Ca^{2+}–O, As^{5+}–O) and from Brown (2002) (H^+–O).

FIGURE 4. Packing of infinite chains in the structure of smamite viewed along (**a**) [100] direction. Notice the short O5–H5–O5 hydrogen bond that provides additional extra-chain linkage. (**b**) In a general direction, approximately parallel to the length of chains. Color scheme is same as in the previous figure. Unit-cell edges are outlined in black solid lines. (Color online.)
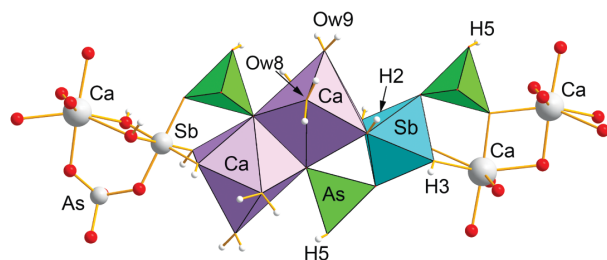

FIGURE 5. Infinite chain found in the structure of smamite. The As-tetrahedra are in green color. (Color online.)

and fluckite (as the main Mn-bearing arsenate).

Weathering of Sb-ores and the fate of Sb in the environment have been much less studied than that of As. A few recent studies have shown that the common products of supergene weathering of primary Sb ores comprise Sb-bearing minerals of the pyrochlore group (stibiconite, roméite, and bindheimite) and tripuhyite, $Fe^{3+}Sb^{5+}O_4$, accompanied often by goethite and hydrous ferric oxide with adsorbed or incorporated Sb (Keim et al. 2018; Majzlan et al. 2018, and references therein). A recently published study on the redistribution of elements during oxidative dissolution of tetrahedrite from Piesky, Slovakia (Majzlan et al. 2018) has documented that ~10% As and almost 50% of Sb (from the initial 100% in primary tetrahedrite) are lost during weathering. Likely, they are being released into water with some Sb stored in the supergene minerals camérolaite, cualstibite, and tripuhyite. According to Majzlan et al. (2018), antimony is more abundant than arsenic in the aqueous fluids, and all contaminated water samples are supersaturated with respect to tripuhyite. In the system, which is overall poor in arsenic, antimony associates

temporarily with Ca or Al but is slowly converted to the "ultimate sink," which is tripuhyite. One can speculate that, in the As-rich environment, which is also rich in Sb, smamite, and other possible new mineral phases in the system Me–Sb^{5+}–AsO_4–H_2O may serve as sinks for Sb, due to their low solubility in aqueous solutions with circumneutral pH (by analogy with smamite).

REFERENCES CITED

Bari, H., Permingeat, F., Pierrot, R., and Walenta, K. (1980a) La ferrarisite, $Ca_5H_2(AsO_4)_4 \times 9H_2O$, une nouvelle espèce minérale isomorphe de la guérinite. Bulletin de la Societé Française de Minéral et de Cristallographie, 103, 533–540.

Bari, H., Cesbron, F., Permingeat, F., and Pillard, F. (1980b) La fluckite, arséniate hydraté de calcium et manganèse, $CaMnH_2(AsO_4)_2 \times 2H_2O$, une nouvelle espèce minérale. Bulletin de la Societé Française de Minéral et de Cristallographie, 103, 122–128.

Bari, H., Catti, M., Ferraris, G., Ivaldi, G., and Permingeat, F. (1982) Phaunouxite, $Ca_3(AsO_4)_2 \times 11H_2O$, a new mineral strictly associated with rauenthalite. Bulletin de la Societé Française de Minéral et de Cristallographie, 105, 327–332.

Borčinová Radková, A., Jamieson, H., Lalinská-Voleková, B., Majzlan, J., Števko, M., and Chovan, M. (2017) Mineralogical controls on antimony and arsenic mobility during tetrahedrite-tennantite weathering at historic mine sites Špania Dolina-Piesky and Ľubietova-Svatodušná, Slovakia. American Mineralogist, 102, 1091–1100.

Brown, I.D. (2002) The Chemical Bond in Inorganic Chemistry: The Bond Valence Model. Oxford University Press.

Đorđević, T., Kolitsch, U., Serafimovski, T., Tasev, G., Tepe, N., Stöger-Pollach, M., Hofmann, T., and Boev, B. (2019) Mineralogy and weathering of realgar-rich tailings at a former As-Sb-Cr mine at Lojane, North Macedonia. Canadian

Mineralogist, 57, 403–423.

Ferraris, G., Jones, D.W., and Yerkess, J. (1971) Symmetrical hydrogen bonds in the crystal structure of calcium bis(dihydrogen arsenate): a neutron-diffraction study. Journal of the Chemical Society D, 23, 1566–1567.

——— (1972) A neutron diffraction study of the crystal structure of calcium bis(dihydrogen arsenate), Ca(H$_2$AsO$_4$)$_2$. Acta Crystallographica, B28, 2430–2437.

Gagné, O.C., and Hawthorne, F.C. (2015) Comprehensive derivation of bond-valence parameters for ion pairs involving oxygen. Acta Crystallographica, B71, 562–578.

Gunter, M.E., Bandli, B.R., Bloss, F.D., Evans, S.H., Su, S.C., and Weaver, R. (2004) Results from a McCrone spindle stage short course, a new version of EXCALIBR, and how to build a spindle stage. The Microscope, 52, 23–39.

Herpin, P., and Pierrot, R. (1963) La weilite, CaH(AsO$_4$), un nouvel arséniate de calcium isomorphe de la monétite. Bulletin de la Societé Française de Minéral et de Cristallographie, 86, 368–372.

Higashi, T. (2001) ABSCOR. Rigaku Corporation, Tokyo.

Keim, M.F., Staude, M., Marquardt, K., Bachmann, K., Opitz, J., and Markl, G. (2018) Weathering of Bi-tennantite. Chemical Geology, 499, 1–25.

Kolitsch, U., Sejkora, J., Topa, D., Kampf, A.R., Plášil, J., Rieck, B., and Fabritz, K.H. (2018) Pracharite, IMA 2018-081. CNMNC Newsletter No. 46, December 2018, page 1183; European Journal of Mineralogy, 30, 1181–1189.

Libowitzky E. (1999) Correlation of O–H stretching frequencies and O–H···O hydrogen bond lengths inminerals. Monatshefte für Chemie, 130, 1047–1059.

Majzlan, J., Plášil, J., Škoda, R., Gescher, J., Kögler, P., Rusznyak, A., Küsel, K., Neu, T.R., Mangold, S., and Rothe, J. (2014) Arsenic-rich acid mine water with extreme arsenic concentration: mineralogy, geochemistry, microbiology, and environmental implications. Environmental Science & Technology, 48, 13685–13693.

Majzlan, J., Kiefer, S., Hermann, J., Števko, M., Sejkora, J., Chovan, M., Láncosz, T., Lazarov, M., Gerdes, A., Langenhorst, F., Borčinová Radková, A., Jamieson, H., and Milovský, R. (2018) Synergies in elemental mobility during weathering of tetrahedrite [(Cu,Fe,Zn)$_{12}$(Sb,As)$_4$S$_{13}$]: Field observations, electron microscopy, isotopes of Cu, C, O, radiometric dating, and water geochemistry. Chemical Geology, 488, 1–20.

Mandarino, J.A. (2007) The Gladstone–Dale compatibility of minerals and its use in selecting mineral species for further study. Canadian Mineralogist, 45, 1307–1324.

Markl, G., Marks, M.A.W., Derrey, I., and Gühring, J.E. (2014) Weathering of cobalt arsenides: natural assemblages and calculated stability relations among secondary Ca–Mg–Co arsenates and carbonates. American Mineralogist, 99, 44–56.

Meisser, N., Plášil, J., Brunsperger, T., Lheur, C., and Škoda, R. (2019) Giftgrubeite, CaMn$_2$Ca$_2$(AsO$_4$)$_2$(AsO$_3$OH)$_2$×4H$_2$O, a new member of the hureaulite group from Sainte-Marie-aux-Mines, Haut-Rhin Department, Vosges, France. Journal of Geosciences, 64, 73–80.

Merlet, C. (1994) An accurate computer correction program for quantitative electron probe microanalysis. Microchimica Acta, 114/115, 363–376.

Mills, S.J., Kolitsch, U., Miyawaki, R., Groat, L.A., and Poirier, G. (2009) Joël-bruggerite, Pb$_3$Zn$_3$(Sb^{5+},Te^{6+})As$_2$O$_{13}$(OH,O), the Sb^{5+} analogue of dugganite, from the Black Pine mine, Montana. American Mineralogist, 94, 1012–1017.

Petríček, V., Dušek, M., and Palatinus, L. (2014) Crystallographic Computing System Jana 2006: general features. Zeitschrift für Kristallographie, 229, 345–352.

Pierrot, R. (1964) Contribution à la minéralogie des arséniates calciques et calcaromagnésiens naturels. Bulletin de la Societé Française de Minéral et de Cristallographie, 87, 169–211.

Sarp, H. (1984) Villyaellenite, H$_2$(Mn,Ca)$_5$(AsO$_4$)$_4$×4H$_2$O un nouveau mineral de Sainte-Marie aux-Mines (France). Schweizerische mineralogishe petrographische Mitteilungen, 64, 323–328.

Sarp, H., Deferne, J., and Liebich, B.W. (1981) La mcnéarite, NaCa$_5$H$_4$(AsO$_4$)$_5$×4H$_2$O, un nouvel arséniate hydraté de calcium et de sodium. Schweizerische mineralogishe petrographische Mitteilungen, 61, 1–6.

Sheldrick, G.M. (2015) Crystal structure refinement with SHELXL. Acta Crystallographica, C71, 3–8.

Süsse, P., and Tillmann, B. (1987) The crystal structure of the new mineral richelsdorfite, Ca$_2$Cu$_5$Sb(Cl/(OH)$_6$/(AsO$_4$)$_4$)×6H$_2$O. Zeitschrift für Kristallographie, 179, 323–334.

Endnote: